

## Vertex function for pion-deuteron-dibaryon coupling

H. G. Dosch

*Institut für Theoretische Physik der Universität, D-6900 Heidelberg, Federal Republic of Germany*

Erasmio Ferreira

*Departamento de Física, Pontifícia Universidade Católica, Rio De Janeiro, 22451 RJ, Brasil*

(Received 3 October 1983)

We calculate the pion-deuteron  $2^+$  dibaryon vertex function and the influence on  $\pi d$  elastic scattering of a strong baryon-baryon interaction in the intermediate state. The general results of our investigation are the following. Near the  $\Delta N$  threshold, the contribution to the  $\pi d B_2$  vertex function is largely dominated by the  $\Delta N$  intermediate state. The vertex function falls off rapidly for energies above the  $\Delta N$  threshold. The coupling of a possible  $2^+$  dibaryon resonance at 2.15 GeV to the  $\pi d$  system occurs mainly in an  $l=1$  wave. We evaluate the contributions to  $\pi d$  helicity scattering amplitudes due to explicit  $\Delta N$  interaction in the intermediate state.

### I. INTRODUCTION

The recent investigations on dibaryon resonances have brought additional motivation to the study of pion deuteron processes, where dibaryonic states of appropriate quantum numbers can be formed. The  $\pi$ -d system provides a convenient laboratory for investigations about the existence and properties of dibaryonic states, while, on the other hand, the properties of these states may become essential ingredients of the basic  $\pi$ -d three-body calculations.

Among the dibaryon candidates with isospin 1, the one with quantum numbers  $J^P=2^+$  and mass 2.15 GeV (Ref. 1) is the most intriguing one, and has had a remarkable influence in the interpretation of polarized proton experiments.<sup>2</sup> The proximity between the  $\Delta N$  threshold and the mass value attributed to this state makes it difficult to distinguish between threshold effects and structures expected to arise from the existence of a resonance. Coupled channel analyses<sup>3,4</sup> of the NN,  $\Delta N$ , and  $\Delta\Delta$  systems indicate that this dibaryon state is a true resonance and not an  $\Delta N$  threshold effect. The analysis of Ref. 3 also provides the important information that this dibaryonic state is strongly coupled to the  $\Delta N$  channel. Our investigations show that the influence of a state near  $\Delta N$  threshold is kinematically enhanced in  $\pi$ -d scattering, and therefore in this paper we concentrate on this  $J^P=2^+$  state at 2.15 GeV.

The possibility of a strong  $\Delta N$  interaction near threshold and its kinematical enhancement shows how important  $\Delta N$  dynamics may be in the treatment of the  $\pi$ -d system. As long as the  $\Delta$  resonance is not treated independently and explicitly in the description of the  $\pi$ -d system, but only enters therein through its effects on the  $\pi$ -N interaction, some possibly important contributions of the  $\Delta N$  interaction are being left out. To recover at least part of the loss, contributions representing the  $\Delta N$  interaction, which should account for the formation of dibaryon resonances, must be added directly to the amplitudes obtained in the three-body calculations of the  $\pi$ -d system<sup>5</sup> (hereafter referred to as "background amplitudes"). In attempts

to improve the description of  $\pi$ -d data, several papers<sup>6</sup> have discussed the contributions of dibaryon resonances to be added to the background three-body amplitudes. In these attempts, arbitrary point interactions are assumed to couple the  $\pi$ -d and the dibaryon systems. The coupling strengths are chosen so as to fit the experimental data optimally. Despite the *ad hoc* procedure and the arbitrariness of the coupling constants, the success of these attempts is not impressive.

A dynamical scheme for these couplings is certainly essential for the progress of our understanding of the influence of dibaryon resonances on  $\pi$ -d observables. If dibaryons are states like the deuteron, consisting of two fairly defined baryons, the skeleton diagram of Fig. 1 gives an adequate description of the coupling of the  $\pi$ -d system to the dibaryon state. The present work aims at the study of the consequences of this coupling mechanism, which describes the pion-deuteron-dibaryon ( $B_2$ ) vertex in terms of the deuteron wave function and of the  $\pi NN$ ,  $\pi N\Delta$ ,  $NNB_2$ , and  $N\Delta B_2$  vertices.

In Secs. II–IV we study the  $\pi dB_2$  vertex function derived from this model. In order to exhibit some major features determined by the structure of the triangle diagram and by the values of the masses involved, we first study in Sec. II a model where all particles have realistic masses, but are treated as scalars. This simple model calculation already shows the important result that the diagram where line 3 of Fig. 1 represents a  $\Delta$  propagator is strongly enhanced near the  $\Delta N$  threshold (ca. 2.17 GeV), and dominates over the corresponding diagram where line 3 represents a nucleon propagator, by more than one order of magnitude. We note that this suppression is due to the  $D$ -wave coupling of the two intermediate nucleons to the dibaryon state. The kinematical effects show also that, for reasonable magnitudes of their couplings to the  $\Delta N$  and NN systems, other dibaryon states of higher masses lead to  $\pi dB_2$  vertex functions of smaller magnitudes. This agrees with the results obtained by Matsuyama and Yazaki<sup>7</sup> in a different approach.

In Sec. III we develop the complete formalism which

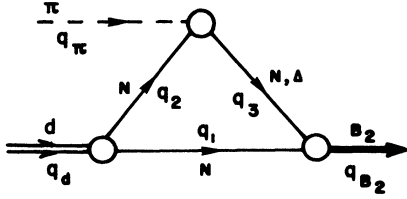


FIG. 1. Skeleton diagrams for the pion-deuteron-dibaryon vertex functions, which are evaluated for the  $J^P=2^+$  dibaryonic state. The diagram with the intermediate  $\Delta$  state is shown to be dominant over the diagram with nucleon lines only.

leads to the evaluation of the  $\pi dB_2$  vertex function, where  $B_2$  is a  $J^P=2^+$  state, assumed to couple to the  $\Delta N$  system in an  $S$  wave. In that section the deuteron is described by an  $S$ - and  $D$ -wave function determined by the five-pole fit of Ref. 8.

In Sec. IV we give the result for the vertex function in the case where the dibaryon is coupled to a  $^1D_2$  two-nucleon state. Since in the energy range of interest the contributions of this diagram to the full vertex function are much smaller than those with an intermediate  $\Delta$ , we use here only a pure  $S$ -wave deuteron wave function.

In Sec. V we study the consequences for elastic  $\pi$ - $d$  scattering of the strong  $\Delta N$  interaction in the intermediate state. The same considerations leading us to the vertex functions of Secs. II–IV show that the contribution of the  $J^P=2^+$  dibaryonic interaction can be represented by the skeleton diagram of Fig. 2. The evaluation of the amplitudes corresponding to this diagram is based on the results of Sec. III. As explained before, as long as the  $\pi d$  interaction is not treated through four-body equations including the  $\Delta$  explicitly, these contributions have to be added to the amplitudes obtained in a conventional three-body calculation of the  $\pi$ - $d$  system. This procedure does not lead to a strong violation of unitarity, since the added contributions are comparatively small. We must remark that the evaluated contributions take into account the full  $S$ -wave  $J=2$  interaction, independently of the existence of a dibaryon resonance in this state. However, if the  $J^P=2^+$ , 2.15 GeV resonance exists, its influence is enhanced due to the proximity of the  $\Delta N$  threshold.

The main results of this paper, namely the  $\pi dB_2$  vertex function and the correction amplitudes to  $\pi$ - $d$  elastic scattering, are self-contained. Phenomenological applications to the evaluation of  $\pi d$  observables will be presented

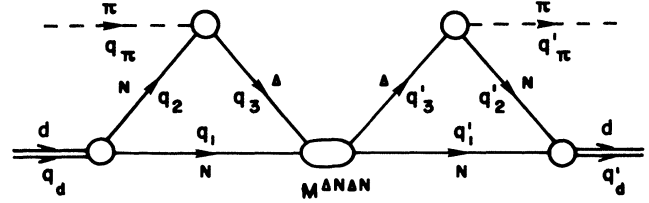


FIG. 2. Skeleton diagram for the contributions to  $\pi d$  elastic scattering due to the  $\Delta N$  interaction in the intermediate state.

in a subsequent paper. A first application to the forward elastic amplitude has already been made.<sup>9</sup>

## II. SCALAR MODEL FOR THE $\pi dB_2$ VERTEX FUNCTION

The present work is based on the assumption that the dibaryonic states are directly connected mostly to two three-quark hadronic states, which can be  $\Delta$ 's or  $N$ 's. The coupling of  $\pi$ - $d$  to the dibaryon system then dominantly occurs through the skeleton diagram of Fig. 1, and  $B_2$  formation takes place after absorption of the pion by one of the nucleons. If the dibaryon mass happens to be near the threshold for one of the directly coupled channels, threshold effects implied by the diagram (generalized unitarity) become particularly important. The characteristic energy dependence caused by these threshold effects is superimposed to the energy dependence induced by the resonance formation (the Breit-Wigner form, e.g.). In this section we wish to exhibit these threshold effects in a neat way, without complications arising from spin variables, and therefore we present the results of a simplified calculation of the triangle diagram in which all particles are scalar. We are thus able to discuss separately some important characteristic features of our treatment of the  $\pi dB_2$  vertex. In the following sections we present the complete and realistic calculation.

We write the amplitude as a sum of two parts,

$$M^{\pi dB_2(s)} = M^{\pi dB_2; N(s)} + M^{\pi dB_2; \Delta(s)}, \quad (2.1)$$

where the last superscript indicates the nature of the baryon which is produced after pion absorption (the line with momentum  $q_3$  in Fig. 1).

In the nucleon case we obtain

$$M^{\pi dB_2; N(s)} = \frac{i^3}{(2\pi)^4} \int d^4q_1 d^4q_2 d^4q_3 \Gamma^{dNN}(q_1^2, q_2^2) \Gamma^{\pi NN}(q_2^2, q_3^2) \tilde{\Gamma}^{NNB_2}(q_1, q_3) \\ \times \frac{2m_N}{q_1^2 - m_N^2 + i\epsilon} \frac{2m_N}{q_2^2 - m_N^2 + i\epsilon} \frac{2m_N}{q_3^2 - m_N^2 + i\epsilon} \delta(q_1 + q_2 - q_d) \delta(q_2 + q_\pi - q_3), \quad (2.2)$$

where  $q_d$  and  $q_\pi$  denote the “deuteron” and pion four-momenta, respectively;  $s$  is the Mandelstam variable  $s = (q_\pi + q_d)^2$ ; and the quantities  $\Gamma^{dNN}(q_1^2, q_2^2)$ ,  $\Gamma^{\pi NN}(q_2^2, q_3^2)$ , and  $\tilde{\Gamma}^{NNB_2}(q_1, q_3)$  represent the  $dNN$ ,  $\pi NN$ , and  $NNB_2$  vertex functions, respectively. We take care of the fact that the dibaryon in the realistic case is

coupled to the two nucleons in a  $D$  state, and therefore make for the  $NNB_2$  vertex function the ansatz

$$\tilde{\Gamma}^{NNB_2}(q_1, q_3) = P_2(\cos\theta_1) \Gamma^{NNB_2}(q_1^2, q_3^2), \quad (2.3)$$

where  $\cos\theta_1$  is the angle between  $q_1$  and a fixed axis (later to be identified with the direction of pion momentum) in

the  $B_2$  rest frame.  $P_2(\cos\theta)$  is the second order Legendre polynomial. It turns out that this angular dependence, which comes out automatically in the realistic case, leads to a strong suppression of the  $\pi dB_2$  vertex with an intermediate nucleon. The evaluation of Eq. (2.2) is done using

$$\begin{aligned} \text{Abs}\hat{M}^{\pi dB_2;N}(s) &= \frac{1}{2i} \frac{i^3}{(2\pi)^4} (2\pi i)^2 (2m_N)^3 \\ &\times \int d^4q_1 \Gamma^{\text{dNN}}[q_1^2, (q_d - q_1)^2] \Gamma^{\pi\text{NN}}[(q_d - q_1)^2, (q_d - q_1 + q_\pi)^2] \\ &\times \Gamma^{\text{NNB}_2}[q_1^2, (q_d - q_1 + q_\pi)^2] \delta(q_1^2 - m_N^2) \theta(q_{10}) \delta[(q_d - q_1 + q_\pi)^2 - m_N^2] \\ &\times \theta(q_{d0} - q_{10} + q_{\pi 0}) P_2(\cos\theta_1) \frac{1}{(q_d - q_1)^2 - m_N^2 + i\epsilon}. \end{aligned} \quad (2.4)$$

For the demonstrative purpose of this section we take as an ansatz that the dNN vertex is determined by the pure  $S$ -wave Hulthén wave function. We thus write

$$\Gamma^{\text{dNN}}(m_N^2, q_2^2) = \frac{-\Gamma_d}{q_2^2 - m_N^2 - 2(\beta^2 - \alpha^2)}, \quad (2.5a)$$

where for  $\Gamma_d$  we chose, for easier comparison with the realistic case, the constant

$$\Gamma_d = 8 \left[ \frac{2\pi\alpha\beta(\alpha+\beta)^3}{m_d} \right]^{1/2}, \quad (2.5b)$$

where

$$\alpha = [m_N(2m_N - m_d)]^{1/2}, \quad \beta = 7\alpha.$$

Since the nearest singularity of  $\Gamma^{\pi\text{NN}}(m_N^2, q_2^2)$  is located at  $q_2^2 = (m_N + m_\pi)^2$ , this vertex function can be approximated by its on-shell value  $\Gamma^{\pi\text{NN}}$ . The  $\delta$  distributions in the integrand of Eq. (2.4) restrict the contributions of

$$\Gamma^{\text{NNB}_2}[q_1^2, (q_d - q_1 + q_\pi)^2]$$

to its on-mass shell value  $\Gamma^{\text{NNB}_2}$ .

The absorptive part of the nucleon case can now be evaluated explicitly, yielding

$$\text{Abs}\hat{M}^{\pi dB_2;N}(s) = \Gamma^{\pi\text{NN}} \Gamma^{\text{NNB}_2} \text{Abs}\hat{M}^N(s), \quad (2.6a)$$

where

$$\begin{aligned} \text{Abs}\hat{M}^N(s) &= -(2m_N)^3 \frac{\Gamma_d}{64\pi(\beta^2 - \alpha^2)} \frac{1}{|\vec{q}_d| \sqrt{s}} \\ &\times \left\{ P_2 \left[ \frac{A_0}{B} \right] \log \frac{A_0 + B}{A_0 - B} - 3 \frac{A_0}{B} \right. \\ &\quad \left. - P_2 \left[ \frac{A_1}{B} \right] \log \frac{A_1 + B}{A_1 - B} + 3 \frac{A_1}{B} \right\} \\ &\times \theta(s - 4m_N^2), \end{aligned} \quad (2.6b)$$

dispersion techniques.<sup>10</sup> The nearest singularity is given by the singularities of the propagators corresponding to lines 2 and 3 in Fig. 1. We neglect the more distant singularities due to the momentum dependence of the vertex functions. The absorptive part is then written

where

$$\begin{aligned} |\vec{q}_d| &= |\vec{q}_\pi| \\ &= \frac{1}{2\sqrt{s}} \{ [s - (m_d + m_\pi)^2] \cdot [s - (m_d - m_\pi)^2] \} \end{aligned} \quad (2.7)$$

is the center of mass momentum of the  $\pi$ -d system. Note that  $|\vec{q}_d|$  is imaginary for  $4m_N^2 < s < (m_d + m_\pi)^2$ .

The quantities  $A_0$ ,  $A_1$ , and  $B$  are determined by

$$\begin{aligned} A_0 &= m_d^2 - 2E_d E_1, \\ A_1 &= A_0 - 2(\beta^2 - \alpha^2), \\ B &= 2|\vec{q}_d| \cdot |\vec{q}_1|, \end{aligned} \quad (2.8a)$$

where

$$E_d = \frac{1}{2\sqrt{s}} (s + m_d^2 - m_\pi^2) \quad (2.8b)$$

is the deuteron energy in the  $\pi$ d c.m. system and  $|\vec{q}_1|$  and  $E_1$  take the values

$$E_1 = \sqrt{s}/2, \quad |\vec{q}_1| = (E_1^2 - m_N^2)^{1/2}. \quad (2.8c)$$

The full amplitude is given by

$$\begin{aligned} M^{\pi dB_2;N}(s) &= \Gamma^{\pi\text{NN}} \Gamma^{\text{NNB}_2} [\text{Disp}\hat{M}^N(s) \\ &\quad + i \text{Abs}\hat{M}^N(s)], \end{aligned} \quad (2.9a)$$

where the dispersive part is given by the principal value integral

$$\text{Disp}\hat{M}^N(s) = \frac{1}{\pi} \int_{4m_N^2}^{\infty} \frac{\text{Abs}\hat{M}^N(s')}{s' - s} ds'. \quad (2.9b)$$

In the evaluation of the amplitude  $M^{\pi dB_2;\Delta}$  for the diagram with an internal  $\Delta$  particle, we follow the same lines as in the nucleon case. We approximate the effects of the  $\Delta$  instability by using a propagator with a complex pole. We thus write

$$M^{\pi dB_2; \Delta}(s) = \frac{i^3}{(2\pi)^4} \int d^4 q_1 d^4 q_2 d^4 q_3 (2m_N)^2 2m_\Delta \frac{\Gamma^{\text{dNN}}(q_1^2, q_2^2) \Gamma^{\pi N \Delta}(q_2^2, q_3^2) \Gamma^{\text{N} \Delta B_2}(q_1^2, q_3^2)}{(q_1^2 - m_N^2 + i\epsilon)(q_2^2 - m_N^2 + i\epsilon)(q_3^2 - m_\Delta^2 + im_\Delta \Gamma_\Delta)} \\ \times \delta(q_1 + q_2 - q_d) \delta(q_2 + q_\pi - q_3), \quad (2.10)$$

where  $m_\Delta$  and  $\Gamma_\Delta$  are the  $\Delta$  mass and width, respectively. Here we have taken an  $S$ -wave  $\text{N} \Delta B_2$  coupling.

As for the nucleon case, we take into account only the absorptive contributions due to the singularities of the propagators for lines 2 and 3 in Fig. 1. We cut the imaginary part of the  $\Delta$  propagator at the  $\text{N}-\pi$  threshold, i.e., we use for the imaginary part of the  $\Delta$  propagator the expression

$$\theta[q_3^2 - (m_N + m_\pi)^2] \frac{m_\Delta \Gamma_\Delta}{(q_3^2 - m_\Delta^2)^2 + m_\Delta^2 \Gamma_\Delta^2}. \quad (2.11)$$

Then,

$$\text{Abs} M^{\pi dB_2; \Delta}(s) = \frac{1}{2i} \frac{i^3}{(2\pi)^4} (2\pi i) (2m_N)^2 2m_\Delta \\ \times \int d^4 q_1 \delta(q_1^2 - m_N^2) \frac{2i \Gamma_\Delta m_\Delta \theta[(q_d - q_1 + q_\pi)^2 - (m_N + m_\pi)^2]}{[(q_d - q_1 + q_\pi)^2 - m_\Delta^2]^2 + m_\Delta^2 \Gamma_\Delta^2} \\ \times \frac{\Gamma^{\text{dNN}}[q_1^2, (q_d - q_1)^2] \Gamma^{\pi N \Delta}[(q_d - q_1)^2, (q_d - q_1 + q_\pi)^2] \Gamma^{\text{N} \Delta B_2}[q_1^2, (q_d - q_1 + q_\pi)^2]}{(q_d - q_1)^2 - m_N^2} \theta(q_{10}) \\ = \frac{1}{2i} (2m_N)^2 2m_\Delta \frac{i^3}{(2\pi)^4} (2\pi i)^2 \int_{(m_N + m_\pi)^2}^\infty d\mu^2 \frac{\Gamma_\Delta m_\Delta / \pi}{(\mu^2 - m_\Delta^2)^2 + \Gamma_\Delta^2 m_\Delta^2} \\ \times \int d^4 q_1 \delta[(q_d - q_1 + q_\pi)^2 - \mu^2] \delta(q_1^2 - m_N^2) \theta(q_{10}) \\ \times \frac{\Gamma^{\text{dNN}}[m_N^2, (q_d - q_1)^2] \Gamma^{\pi N \Delta}[(q_d - q_1)^2, \mu^2]}{(q_d - q_1)^2 - m_N^2} \\ \times \Gamma^{\text{N} \Delta B_2}(m_N^2, \mu^2). \quad (2.12)$$

An auxiliary variable  $\mu^2$  has been introduced in the last part of Eq. (2.12) through the identity

$$\theta[(q_d - q_1 + q_\pi)^2 - (m_N + m_\pi)^2] \\ = \int_{(m_N + m_\pi)^2}^\infty d\mu^2 \delta[\mu^2 - (q_d - q_1 + q_\pi)^2]. \quad (2.13)$$

We again use Eq. (2.5) to fix the form of  $\Gamma^{\text{dNN}}[m_N^2, (q_d - q_1)^2]$ , and approximate  $\Gamma^{\pi N \Delta}[(q_d - q_1)^2, \mu^2]$  and  $\Gamma^{\text{N} \Delta B_2}(m_N^2, \mu^2)$  by their ‘‘on-shell values,’’

$$\Gamma^{\pi N \Delta} \equiv \Gamma^{\pi N \Delta}(m_N^2, m_\Delta^2), \quad (2.14)$$

$$\Gamma^{\text{N} \Delta B_2} \equiv \Gamma^{\text{N} \Delta B_2}(m_N^2, m_\Delta^2).$$

Performing the integrations over  $q_1$ , we obtain

$$\text{Abs} M^{\pi dB_2; \Delta}(s) = \Gamma^{\pi N \Delta} \Gamma^{\text{N} \Delta B_2} \text{Abs} \hat{M}^\Delta(s) \quad (2.15a)$$

with

$$\text{Abs} \hat{M}^\Delta(s) = \frac{-\Gamma_d}{64\pi(\beta^2 - \alpha^2)} \frac{(2m_N)^2 2m_\Delta}{|\vec{q}_d| \sqrt{s}} \\ \times \int_{(m_N + m_\pi)^2}^{(\sqrt{s} - m_N)^2} d\mu^2 \frac{\Gamma_\Delta m_\Delta / \pi}{(\mu^2 - m_\Delta^2)^2 + m_\Delta^2 \Gamma_\Delta^2} \\ \times \left\{ \ln \left[ \frac{A_0 + B}{A_0 - B} \right] - \ln \left[ \frac{A_1 + B}{A_1 - B} \right] \right\}. \quad (2.15b)$$

The functions  $A_0$ ,  $A_1$ , and  $B$  are defined by Eq. (2.8), but for  $E_1$  and  $q_1$  in the intermediate  $\Delta$  case we have

$$E_1 = \frac{s + m_N^2 - \mu^2}{2\sqrt{s}}, \quad |\vec{q}_1| = (E_1^2 - \mu^2)^{1/2}. \quad (2.16)$$

The upper limit in the  $\mu^2$  integration is due to the fact that for fixed  $\mu^2$  the absorptive part starts at  $s = (m_N + \mu)^2$ . We observe that the above integral represents a smearing over the  $\Delta$  mass distribution. The integration over  $\mu^2$  is performed numerically. The full amplitude is again written as

$$M^{\pi d B_2; \Delta}(s) = \Gamma^{\pi N \Delta} \Gamma^{N \Delta B_2} [ \text{Disp} \hat{M}^{\Delta}(s) + i \text{Abs} \hat{M}^{\Delta}(s) ], \quad (2.17a)$$

with

$$\text{Disp} \hat{M}^{\Delta}(s) = \frac{1}{\pi} \int_{(2m_N + m_\pi)^2}^{\infty} \frac{\text{Abs} \hat{M}^{\Delta}(s')}{s' - s} ds'. \quad (2.17b)$$

In Figs. 3 and 4 we display the absorptive and dispersive parts of  $\hat{M}^N(s)$  and  $\hat{M}^{\Delta}(s)$ .

We now note the main features of the vertex functions, which will not be essentially modified in the next section, when more realistic wave functions are used and spin variables included.

(1) The contribution with an internal nucleon line is suppressed, as compared to the contribution with an internal delta line, by more than an order of magnitude in the energy region of our interest, i.e.,  $s \approx (m_N + m_\Delta)^2$ . This suppression is mainly due to the  $D$ -wave coupling [see Eq.

(2.3)] of the nucleons to the dibaryonic state.

(2) Figure 4 shows a strong enhancement of the amplitude for the  $\Delta$  case near the  $\Delta N$  threshold. Since the  $J^P = 2^+$  dibaryon candidate has a mass value resting in this region, we can predict that dibaryon resonances with higher masses would be more weakly coupled to the  $\pi d$  channel.

### III. THE $\pi d B_2$ VERTEX FUNCTION: INTERMEDIATE $\Delta$ CONTRIBUTION

We now perform the complete calculation of the vertex function, taking into account the spin variables and using a complete and more accurate wave function for the deuteron.<sup>8</sup> Since, in the energy range of our interest, the contribution of the diagram with an internal  $\Delta$  line is much more important, we start with the treatment of this case.

The amplitude for the diagram in Fig. 1 is written (doubly occurring indices are to be summed over) as follows:

$$M_{s_d, s_B}^{\pi d B_2; \Delta}(s) = \frac{i^3}{(2\pi)^4} \int d^4 q_1 \xi^{s_d, \lambda} \Gamma_{\lambda; \alpha\beta}^{dNN}(q_1, q_d - q_1) \frac{\Sigma_{\gamma\beta}(q_d - q_1)}{(q_d - q_1)^2 - m_N^2 + i\epsilon} \Gamma_{\gamma; \delta\mu}^{\pi N \Delta}(q_d - q_1, q_d - q_1 + q_\pi) \\ \times \frac{\Lambda_{\epsilon\delta}^{\eta\alpha}(q_d - q_1 + q_\pi)}{(q_d - q_1 + q_\pi)^2 - m_\Delta^2 + im_\Delta \Gamma_\Delta} \frac{\Sigma_{\eta\alpha}(q_1)}{q_1^2 - m_N^2 + i\epsilon} \Gamma_{\rho\sigma; \epsilon\nu\eta}^{N \Delta B_2}(q_1, q_d - q_1 + q_\pi) R^{\rho\sigma, s_B}, \quad (3.1)$$

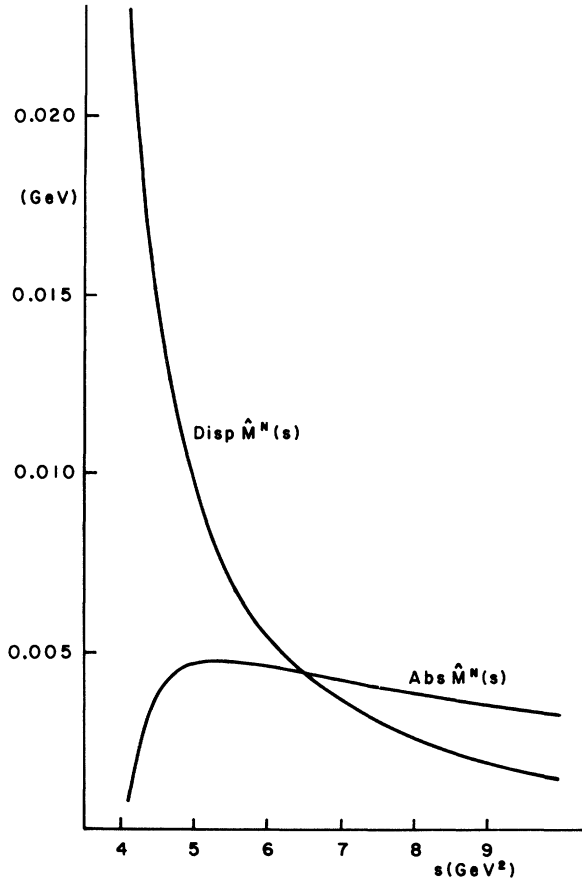


FIG. 3. Absorptive and dispersive parts of the vertex function in the scalar model calculation for the diagram of Fig. 1 with nucleon lines only. The plotted quantities are defined through Eqs. (2.6)–(2.9).

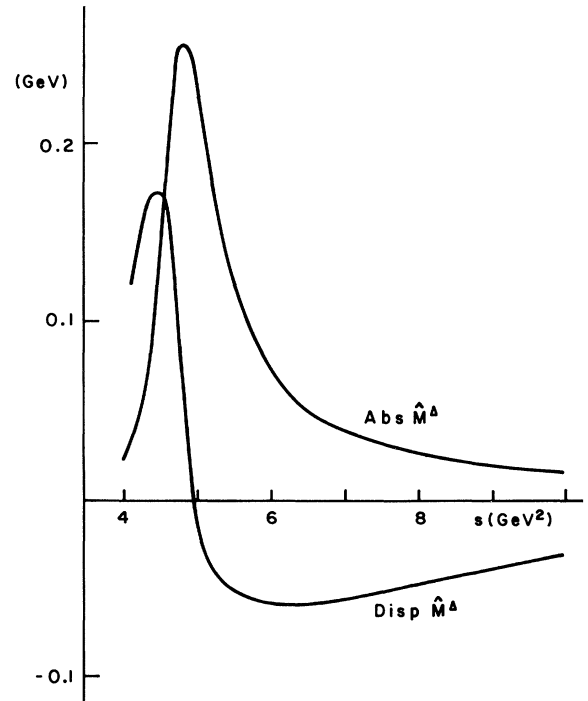


FIG. 4. Absorptive and dispersive parts of the vertex function in the scalar model calculation for the diagram of Fig. 1 with a  $\Delta$  resonance in line 3. The plotted quantities are defined through Eqs. (2.15)–(2.17).

where  $\vec{\xi}^{sd}$  represents the deuteron polarization vector;  $\Sigma_{\gamma\beta}(q_1)$  and  $\Lambda_{\epsilon\delta}^{\mu\nu}(q_3)$  are the usual numerators of the spin  $\frac{1}{2}$  and  $\frac{3}{2}$  propagators, respectively; while  $\Gamma^{\text{dNN}}$ ,  $\Gamma^{\pi\text{N}\Delta}$ , and  $\Gamma^{\text{N}\Delta B_2}$  are the reduced dNN,  $\pi\text{N}\Delta$ , and  $\text{N}\Delta B_2$  vertex functions, respectively. These vertex functions are related to the corresponding full vertex amplitudes through

$$M_{s_d; s_1 s_2}^{\text{dNN}}(q_1, q_2) = \Gamma_{\lambda; \alpha\beta}^{\text{dNN}}(q_1, q_2) \bar{u}_\alpha^{s_1}(q_1) \bar{u}_\beta^{s_2}(q_2) \xi^{sd, \lambda}, \quad (3.2)$$

$$M_{s_3 s_2}^{\pi\text{N}\Delta}(q_2, q_2 + q_\pi) = \Gamma_{\gamma; \delta\mu}^{\pi\text{N}\Delta}(q_2, q_2 + q_\pi) \bar{u}_\delta^{\mu s_3}(q_2 + q_\pi) u_\gamma^{s_2}(q_2),$$

and

$$M_{s_1 s_3; s_B}^{\text{N}\Delta B_2}(q_1, q_3) = \Gamma_{\rho\sigma; \epsilon\eta}^{\text{N}\Delta B_2}(q_1, q_3) u_\eta^{s_1}(q_1) u_\epsilon^{vs_3}(q_3) R^{\rho\sigma; s_B}.$$

Here  $u_\alpha^s(q)$  is a Dirac spinor,  $u_\epsilon^{\mu s}(q)$  is a spin  $\frac{3}{2}$  Rarita-Schwinger spinor, and  $R^{\rho\sigma; s}$  represents the polarization tensor of a spin-2 particle. In each of these cases the superscript  $s$  denotes the magnetic spin quantum number.

We express  $M_{s_d; s_B}^{\pi\text{d}B_2; \Delta}(s)$  in terms of the full vertex amplitudes, which are assumed to vary slowly when extended off their mass shells. For this purpose we use the relations

$$\Sigma_{\alpha\beta}(q) = 2m_N \sum_{s=-1/2}^{+1/2} u_\alpha^s(q) \bar{u}_\beta^s(q), \quad (3.3a)$$

$$\Lambda_{\alpha\beta}^{\mu\nu}(q) = 2m_\Delta \sum_{s=-3/2}^{+3/2} u_\alpha^{\mu s}(q) u_\beta^{\nu s}(q). \quad (3.3b)$$

We then combine the spinors with the vertex functions to form the invariant amplitudes, and obtain

$$\begin{aligned} M_{s_d; s_B}^{\pi\text{d}B_2; \Delta}(s) &= \frac{i^3}{(2\pi)^4} (2m_N)^2 2m_\Delta \\ &\times \int d^4 q_1 \sum_{s_1 s_2 s_3} M_{s_d; s_1 s_2}^{\text{dNN}}(q_1, q_d - q_1) M_{s_2 s_3}^{\pi\text{N}\Delta}(q_d - q_1, q_d - q_1 + q_\pi) M_{s_1 s_3; s_B}^{\text{N}\Delta B_2}(q_1, q_d - q_1 + q_\pi) \\ &\times \frac{1}{(q_1^2 - m_N^2 + i\epsilon)[(q_d - q_1)^2 - m_N^2 + i\epsilon][(q_d - q_1 + q_\pi)^2 - m_\Delta^2 + i\Gamma_\Delta m_\Delta]}. \end{aligned} \quad (3.4)$$

Similarly as in the preceding section, we take into account only the absorptive contribution of the singularities due to the internal lines 1 and 3. We then obtain

$$\begin{aligned} \text{Abs} M_{s_d; s_B}^{\pi\text{d}B_2; \Delta}(s) &= \frac{i^3}{2i} \frac{(2\pi i)^2}{(2\pi)^4} (2m_N)^2 2m_\Delta \\ &\times \int_{(m_N + m_\pi)^2}^{(\sqrt{s} - m_N)^2} d\mu^2 \frac{\Gamma_\Delta m_\Delta / \pi}{(\mu^2 - m_\Delta^2)^2 + \Gamma_\Delta^2 m_\Delta^2} \\ &\times \int d^4 q_1 \delta(q_1^2 - m_N^2) \theta(q_{10}) \delta[(q_d - q_1 + q_\pi)^2 - \mu^2] \frac{1}{(q_d - q_1)^2 - m_N^2} \\ &\times \sum_{s_1 s_2 s_3} M_{s_d; s_1 s_2}^{\text{dNN}}(q_1, q_d - q_1) M_{s_2 s_3}^{\pi\text{N}\Delta}(q_d - q_1, q_d - q_1 + q_\pi) \\ &\times M_{s_1 s_3; s_B}^{\text{N}\Delta B_2}(q_1, q_d - q_1 + q_\pi). \end{aligned} \quad (3.5)$$

We extract  $M^{\pi\text{N}\Delta}(q_d - q_1, q_d - q_1 + q_\pi)$  from the integral at the values  $(q_d - q_1)^2 = m_N^2$  and  $\mu^2 = m_\Delta^2$  and then introduce explicit expressions for the vertex amplitudes. For the dNN vertex amplitude we use a generalization of the Hulthén wave function including  $S$  and  $D$  waves:

$$\begin{aligned} M_{s_d; s_1 s_2}^{\text{dNN}}[m_N^2, (q_d - q_1)^2] &= \chi^{s_1} \left\{ F_S[(q_d - q_1)^2] (\vec{\sigma} \cdot \vec{\xi}^{sd}) \right. \\ &\quad \left. + \frac{3}{\sqrt{2}} F_D[(q_d - q_1)^2] \left[ \frac{(\vec{\sigma} \cdot \vec{q}')(\vec{q}' \cdot \vec{\xi}^{sd})}{|\vec{q}'|^2} - \frac{1}{3} (\vec{\sigma} \cdot \vec{\xi}^{sd}) \right] \right\} \chi^{s_2}. \end{aligned} \quad (3.6)$$

Here all three-vectors refer to the deuteron rest frame, with  $\vec{q}'$  representing the nucleon momentum.

The  $\pi\text{N}\Delta$  coupling is of the form

$$M_{s_2 s_3}^{\pi N \Delta}(m_N^2, m_\Delta^2) = g_{\pi N \Delta} \langle \frac{1}{2} 1; T_2 T_\pi | \frac{1}{2} 1; \frac{3}{2} T_3 \rangle \sum_{s' s''} \langle \frac{1}{2} 1; s' s'' | \frac{1}{2} 1; \frac{3}{2} s_3 \rangle \chi^{s'} \chi^{s''} (\vec{\xi}^{\Delta s''} \cdot \vec{q}^+). \quad (3.7)$$

Here the three-vectors refer to the rest frame of the  $\Delta$ . The quantities  $T_1$ ,  $T_\pi$ , and  $T_3$  are the third components of the  $N$ ,  $\pi$ , and  $\Delta$  isospins, respectively. The  $N\Delta$  coupling to a  ${}^5S_2$ ,  $I=1$  state is written as

$$M_{s_1 s_3; s_B}^{N \Delta B_2}(m_N^2, m_\Delta^2) = g_{N \Delta B_2} \langle \frac{1}{2} \frac{3}{2}; T_1 T_3 | \frac{1}{2} \frac{3}{2}; 1 T_B \rangle \sqrt{4/3} \sum_{s' s''} \langle \frac{1}{2} 1; s' s'' | \frac{1}{2} 1; \frac{3}{2} s_3 \rangle [\chi^{s'} (-i\sigma_2) \sigma_k \chi^{s''}] \xi_l^{\Delta s''} R_{kl}^{s_B}, \quad (3.8)$$

where now the vectors refer to the  $\pi d$  rest frame. The factor  $\sqrt{4/3}$  is introduced for convenience;  $R_{kl}^{s_B}$  is a traceless symmetric  $3 \times 3$  tensor describing a spin-2 particle in its rest frame. We observe that, due to the spin 2 of the dibaryon state, only the spin  $\frac{3}{2}$  part of the product  $\chi^{s'} \xi_l^{\Delta s''}$  contributes, and therefore the Clebsch-Gordan coefficients in (3.7) and (3.8) can be ignored when the spin sums are performed.

Performing the spin and isospin summations in Eq. (3.5), we obtain

$$\begin{aligned} \text{Abs} M_{s_d, s_B}^{\pi d B_2}(s) &= \frac{i^3}{2i} \frac{(2\pi i)^2}{(2\pi)^4} (2m_N)^2 2m_\Delta \\ &\times \int_{(m_N+m_\pi)^2}^{\infty} d\mu^2 \frac{\Gamma_\Delta m_\Delta / \pi}{(\mu^2 - m_\Delta^2)^2 + \Gamma_\Delta^2 m_\Delta^2} \\ &\times \int d^4 q_1 \frac{\delta(q_1^2 - m_N^2)}{(q_d - q_1)^2 - m_N^2} \theta(q_{10}) \delta[(q_d - q_1 + q_\pi)^2 - \mu^2] g_{\pi N \Delta} g_{N \Delta B_2} \frac{4}{3} R_{kl}^{s_B} \\ &\times \left\{ \left[ F_S((q_d - q_1)^2) - \frac{1}{\sqrt{2}} F_D((q_d - q_1)^2) \right] (q_\pi^+)_k \xi_l^{s_d} \right. \\ &\quad \left. + \frac{3}{\sqrt{2}} F_D((q_d - q_1)^2) \frac{\vec{q}' \cdot \vec{\xi}^{s_d}}{|\vec{q}'|^2} (q_\pi^+)_k q_l^i \right\}. \quad (3.9) \end{aligned}$$

We must remember that  $\vec{q}_\pi^+$  is the pion momentum in the  $\Delta$  rest frame, while  $\vec{q}'$  is the nucleon momentum in the deuteron rest frame.

Convenient expressions for  $F_S$  and  $F_D$  are given by the pole fit of McGee,<sup>8</sup> namely,

$$F_S(q^2) = -N_d \sum_{i=0}^n \frac{c_i}{q^2 - m_i^2} (q^2 - m_N^2),$$

with

$$\begin{aligned} m_i^2 &= m_N^2 + 2(\beta_i^2 - \beta_0^2), \\ \beta_0 &= \alpha, \quad c_0 = 1, \\ N_d^2 &= \frac{16\pi}{m_d} \left\{ \sum_{k,l=0}^n \frac{c_k c_l}{\beta_k + \beta_l} \right\}^{-1}, \end{aligned} \quad (3.10a)$$

and

$$F_D(q^2) = -\rho N_d \sum_{i=0}^n \frac{c'_i}{q^2 - m_i'^2} (q^2 - m_N^2), \quad (3.10b)$$

with

$$m_i'^2 = m_N^2 + 2(\beta_i'^2 - \beta_0'^2), \quad c'_0 = 1.$$

Numerical values for  $c_i$ ,  $c'_i$ ,  $\beta_i$ ,  $\beta'_i$ , and  $\rho$  from Ref. 8 are given in Table I.

We insert these expressions for  $F_S$  and  $F_D$  into Eq. (3.9), perform the integration over  $q_{10}$  and  $|\vec{q}_1|$  in the  $\pi$ -d c.m. system, and obtain

TABLE I. Parameters of the McGee wave function.  $\beta_0 = \beta'_0 = 0.04613$  GeV;  $c_0 = c'_0 = 1$ ;  $\rho = 0.0269$ .

$j$	$S$ state		$D$ state	
	$\beta_j$	$c_j$	$\beta'_j$	$c'_j$
1	$5.733\beta_0$	$-0.63608$	$4.833\beta_0$	$-20.34$
2	$12.844\beta_0$	$-6.6150$	$10.447\beta_0$	$-36.60$
3	$17.331\beta_0$	$15.2162$	$14.506\beta_0$	$-123.02$
4	$19.643\beta_0$	$-8.9651$	$16.868\beta_0$	$305.11$
5		$0.0$	$21.154\beta_0$	$-126.16$

$$\begin{aligned}
\text{Abs}M_{s_d, s_B}^{\pi dB_2; \Delta}(s) &= \frac{i^3}{2i} \frac{(-2\pi i)^2}{(2\pi)^4} (2m_N)^2 2m_\Delta \frac{4}{3} g_{\pi N \Delta} g_{N \Delta B} \\
&\times 2R_{kl}^{s_B} \int_{(m_N+m_\pi)^2}^{(\sqrt{s}-m_N)^2} d\mu^2 \frac{m_\Delta \Gamma_\Delta / \pi}{(\mu^2 - m_\Delta^2) + m_\Delta^2 \Gamma_\Delta^2} \frac{|\vec{q}_1|}{4\sqrt{s}} \\
&\times \int d\Omega_{\vec{q}_1} (-N_d) \sum_{i=0}^n \left\{ \left[ \frac{c_i}{(m_d^2 + m_N^2 - m_i^2) - 2E_1 E_d + 2|\vec{q}_1| |\vec{q}_d| \cos\theta} \right. \right. \\
&\quad \left. \left. - \frac{\rho}{\sqrt{2}} \frac{c'_i}{(m_d^2 + m_N^2 - m_i'^2) - 2E_1 E_d + 2|\vec{q}_1| |\vec{q}_d| \cos\theta} \right] \right. \\
&\quad \times (q_\pi^+)_k \xi_l^{s_d} + \frac{3\rho}{\sqrt{2}} \frac{c'_i}{(m_d^2 + m_N^2 - m_i'^2) - 2E_1 E_d + 2|\vec{q}_1| |\vec{q}_d| \cos\theta} \\
&\quad \left. \times \frac{(\vec{q}' \cdot \vec{\xi}^{s_d}) (q_\pi^+)_k q_l}{|\vec{q}'|^2} \right\}, \tag{3.11}
\end{aligned}$$

with

$$\begin{aligned}
E_1 &= \frac{1}{2\sqrt{s}} (s + m_N^2 - \mu^2), \quad |\vec{q}_1| = (E_1^2 - m_N^2)^{1/2}, \\
E_d &= \frac{1}{2\sqrt{s}} (s + m_d^2 - \mu^2), \quad |\vec{q}_d| = (E_d^2 - m_d^2)^{1/2}.
\end{aligned} \tag{3.12}$$

Since we are interested in a kinetic energy region which is small compared to the nucleon mass, we may safely use Galilei transformations between the different frames of Eqs. (3.7) and (3.8), i.e., we may use

$$\vec{q}_\pi^+ = \vec{q}_\pi + \frac{s + m_\pi^2 - m_d^2}{s + m_\Delta^2 - m_N^2} \vec{q}_1 \tag{3.13a}$$

and

$$\vec{q}' = \vec{q}_1 - \frac{1}{2} \vec{q}_d. \tag{3.13b}$$

Inserting these relations into Eq. (3.11), we obtain six different types of angular integrals. We write

$$\text{Abs}M_{s_d, s_B}^{\pi dB_2}(s) = -\frac{4}{3} g_{\pi N \Delta} g_{N \Delta B} R_{kl}^{s_B} \int_{(m_N+m_\pi)^2}^{(\sqrt{s}-m_N)^2} d\mu^2 \frac{\Gamma_\Delta m_\Delta / \pi}{(\mu^2 - m_\Delta^2)^2 + m_\Delta^2 \Gamma_\Delta^2} \sum_{j=1}^6 \mathcal{F}_{kl}^j(\mu^2, s), \tag{3.14}$$

with

$$\begin{aligned}
\mathcal{F}_{kl}^1(\mu^2, s) &= P (q_\pi)_k \xi_l^{s_d} \sum_{i=0}^n c_i \int \frac{B d \cos\theta}{A_i^s + B \cos\theta}, \\
\mathcal{F}_{kl}^2(\mu^2, s) &= P \frac{E_\pi}{E_\Delta} \xi_l^{s_d} \sum_{i=0}^n c_i \int \frac{q_{1k} B d \cos\theta}{A_i^s + B \cos\theta}, \\
\mathcal{F}_{kl}^3(\mu^2, s) &= P \left[ \frac{-\rho}{\sqrt{2}} \right] (q_\pi)_k \xi_l^{s_d} \sum_{i=0}^n c'_i \int \frac{B d \cos\theta}{A_i^D + B \cos\theta}, \\
\mathcal{F}_{kl}^4(\mu^2, s) &= P \left[ \frac{-\rho}{\sqrt{2}} \right] \frac{E_\pi}{E_\Delta} \xi_l^{s_d} \sum_{i=0}^n c'_i \int \frac{q_{1k} B d \cos\theta}{A_i^D + B \cos\theta}, \\
\mathcal{F}_{kl}^5(\mu^2, s) &= P \frac{3\rho}{\sqrt{2}} (q_\pi)_k \sum_{i=0}^n c'_i \int \frac{\left[ q_1 - \frac{q_d}{2} \right]_l \left[ \left[ \vec{q}_1 - \frac{\vec{q}_d}{2} \right] \cdot \vec{\xi}^{s_d} \right] B d \cos\theta}{[A_i^D + B \cos\theta] \cdot [A' + B' \cos\theta]}, \\
\mathcal{F}_{kl}^6(\mu^2, s) &= P \frac{3\rho}{\sqrt{2}} \frac{E_\pi}{E_\Delta} \sum_{i=0}^n c'_i \int \frac{q_{1k} \left[ q_1 - \frac{q_d}{2} \right]_l \left[ \left[ \vec{q}_1 - \frac{\vec{q}_d}{2} \right] \cdot \vec{\xi}^{s_d} \right] B d \cos\theta}{[A_i^D + B \cos\theta] \cdot [A' + B' \cos\theta]}.
\end{aligned} \tag{3.15}$$

In the above expression insert

$$\begin{aligned}
P &= N_d m_\Delta m_N^2 \frac{1}{2\pi\sqrt{s} |\vec{q}_d|}, \\
A_i^S &= m_d^2 + m_N^2 - 2E_d E_1 - m_i^2, \\
A_i^D &= m_d^2 + m_N^2 - 2E_d E_1 - m_i'^2, \\
B &= 2 |\vec{q}_1| \cdot |\vec{q}_d|, \quad B' = -B/2, \\
A' &= |\vec{q}_1|^2 + \frac{1}{4} |\vec{q}_d|^2, \\
E_\pi/E_\Delta &= (s + m_\pi^2 - m_d^2)/(s + m_\Delta^2 - \mu^2).
\end{aligned} \tag{3.16}$$

$\mathcal{F}_{kl}^1$  is by far the most important of these terms.  $\mathcal{F}_{kl}^2$  reflects the influence of the Fermi motion on the  $\pi N\Delta$  coupling, and  $\mathcal{F}_{kl}^3, \mathcal{F}_{kl}^4, \mathcal{F}_{kl}^5, \mathcal{F}_{kl}^6$  are proportional to the  $D$ -state admixture of the deuteron. After having performed the angular integrations, the absorptive part takes the form

$$\text{Abs} M_{s_d, s_B}^{\pi d B_2, \Delta}(s) = \frac{4}{3} g_{\pi N \Delta} g_{N \Delta B_2} 2R_{kl}^{s_B} \left\{ \text{Abs} M^{\Delta, 1}(s) (q_\pi)_k \xi_l^{s_d} + \text{Abs} M^{\Delta, 2}(s) \frac{(q_\pi)_k (q_\pi)_l}{|\vec{q}_\pi|^2} (\vec{q}_\pi \cdot \vec{\xi}^{s_d}) \right\}, \tag{3.17a}$$

where we have introduced the two independent vertex functions  $M^{\Delta, 1}(s)$  and  $M^{\Delta, 2}(s)$  for the  $\Delta$  diagram. They are given by

$$\text{Abs} M^{\Delta, j}(s) = -\frac{1}{2} \int_{(m_N + m_\pi)^2}^{(\sqrt{s} - m_N)^2} d\mu^2 \frac{\Gamma_\Delta m_\Delta / \pi}{(\mu^2 - m_\Delta^2)^2 + \Gamma_\Delta^2 m_\Delta^2} G^j(\mu^2, s), \quad j = 1, 2, \tag{3.17b}$$

with

$$\begin{aligned}
G^1(\mu^2, s) &= P \sum_{i=0}^n \left\{ c_i I_0(A_i^S, B) - \frac{\rho}{\sqrt{2}} c_i' I_0(A_i^D, B) + \frac{3\rho}{\sqrt{2}} \frac{2c_i'}{2A' + A_i^D} \left[ \frac{1}{2} + \frac{1}{4} \frac{E_\pi}{E_\Delta} \right] |\vec{q}_1|^2 \right. \\
&\quad \times [-I_2(A_i^D, B) + I_0(A_i^D, B) + I_2(A', B') - I_0(A', B')] \\
&\quad + \frac{E_\pi}{E_\Delta} \frac{|\vec{q}_1|}{|\vec{q}_\pi|} \left\{ -c_i I_1(A_i^S, B) + \frac{\rho}{\sqrt{2}} c_i' I_1(A_i^D, B) + \frac{3\rho}{\sqrt{2}} \frac{2c_i'}{2A' + A_i^D} |\vec{q}_1|^2 \right. \\
&\quad \left. \left. \times [I_3(A_i^D, B) - I_1(A_i^D, B) - I_3(A', B') + I_1(A', B')] \right\} \right\} \tag{3.18}
\end{aligned}$$

and

$$\begin{aligned}
G^2(\mu^2, s) &= P \frac{3\rho}{\sqrt{2}} |\vec{q}_\pi|^2 \sum_{i=0}^n \frac{2c_i'}{2A' + A_i^D} \left\{ \frac{1}{4} [I_0(A_i^D, B) - I_0(A', B')] + \left[ 1 + \frac{E_\pi}{E_\Delta} \right] \frac{1}{2} \frac{|\vec{q}_1|^2}{|\vec{q}_\pi|^2} \right. \\
&\quad \times [3I_2(A_i^D, B) - I_0(A_i^D, B) - 3I_2(A', B') + I_0(A', B')] \\
&\quad - \frac{|\vec{q}_1|}{|\vec{q}_\pi|} \left[ 1 + \frac{1}{4} \frac{E_\pi}{E_\Delta} \right] [I_1(A_i^D, B) - I_1(A', B')] \\
&\quad \left. + \frac{E_\pi}{E_\Delta} \frac{|\vec{q}_1|^3}{|\vec{q}_\pi|^3} \frac{1}{2} [-5I_3(A_i^D, B) + 3I_1(A_i^D, B) + 5I_3(A', B') - 3I_3(A', B')] \right\}. \tag{3.19}
\end{aligned}$$

The expressions

$$\begin{aligned}
I_0(A, B) &= \log \frac{A+B}{A-B}, \quad I_1(A, B) = 2 - \frac{A}{B} I_0(A, B), \\
I_2(A, B) &= \left[ \frac{A}{B} \right]^2 I_0(A, B) - 2 \left[ \frac{A}{B} \right], \quad I_3(A, B) = - \left[ \frac{A}{B} \right]^3 I_0(A, B) + 2 \left[ \frac{A}{B} \right]^2 + \frac{2}{3},
\end{aligned} \tag{3.20}$$

result from the angular integrations. The integrations over  $\mu^2$  are performed numerically.

Finally we obtain for the full vertex amplitude with an intermediate  $\Delta$

$$M_{s_d, s_B}^{\pi d B_2; \Delta}(s) = 2 \frac{4}{3} g_{\pi N \Delta} g_{N \Delta B_2} R_{kl}^{s_B} \left\{ M^{\Delta, 1}(s) (q_\pi)_k \xi_l^{s_d} + M^{\Delta, 2}(s) \frac{(q_\pi)_k (q_\pi)_l}{|\vec{q}_\pi|^2} (\vec{q}_\pi \cdot \vec{\xi}^{s_d}) \right\}. \quad (3.21)$$

$M^{\Delta, j}(s)$  consists of absorptive and dispersive parts,

$$M^{\Delta, j}(s) = \text{Disp} M^{\Delta, j}(s) + i \text{Abs} M^{\Delta, j}(s), \quad j = 1, 2, \quad (3.22a)$$

with

$$\text{Disp} M^{\Delta, j}(s) = \frac{1}{\pi} \int_{(2m_N + m_\pi)^2}^{\infty} \frac{\text{Abs} M^{\Delta, j}(s')}{s' - s} ds'. \quad (3.22b)$$

In Figs. 5 and 6 we display the absorptive and dispersive parts of  $M^{\Delta, 1}(s)$  and  $M^{\Delta, 2}(s)$ . In the energy region of interest the amplitude  $M^{\Delta, 1}(s)$  is larger than  $M^{\Delta, 2}(s)$  by an order of magnitude. This implies that the coupling of  $B_2$  to an  $l=1$   $\pi$ -d wave is much larger than the coupling to the  $l=3$   $\pi$ -d wave.

#### IV. THE $\pi d B_2$ VERTEX FUNCTION: INTERMEDIATE N CONTRIBUTION

In this section we present the  $\pi d B_2$  vertex function for the case where line 3 in diagram 1 is a nucleon line. Since this amplitude is strongly suppressed kinematically, we give the results for a pure  $S$ -wave deuteron wave function. The expression corresponding to Eq. (3.4) is now

$$M_{s_d, s_B}^{\pi d B_2; N}(s) = i^3 (2m_N)^3 \frac{1}{(2\pi)^4} \int d^4 q_1 \sum_{s_1 s_2 s_3} M_{s_d; s_1 s_2}^{\text{dNN}}(q_1, q_d - q_1) \times M_{s_2 s_3}^{\pi NN}(q_d - q_1, q_d - q_1 + q_\pi) M_{s_1 s_3; s_B}^{\text{NN}B_2}(q_1, q_d - q_1 + q_\pi) \times \frac{1}{(q_1^2 - m_N^2 + i\epsilon)[(q_d - q_1)^2 - m_N^2 + i\epsilon][(q_d - q_1 + q_\pi)^2 - m_N^2 + i\epsilon]}. \quad (4.1)$$

Here we are interested in the coupling of the two nucleons in a  $^1D_2$  state; hence, we use

$$M_{s_1 s_3; s_B}^{\text{NN}B_2}(q_1, q_3) = g_{\text{NN}B_2} \langle \frac{1}{2} \frac{1}{2}; T_1 T_2 | \frac{1}{2} \frac{1}{2}; 1 T_B \rangle [\chi^{s_1}(-i\sigma_2) \chi^{s_3}] q_k q_l R_{kl}^{s_B}, \quad (4.2)$$

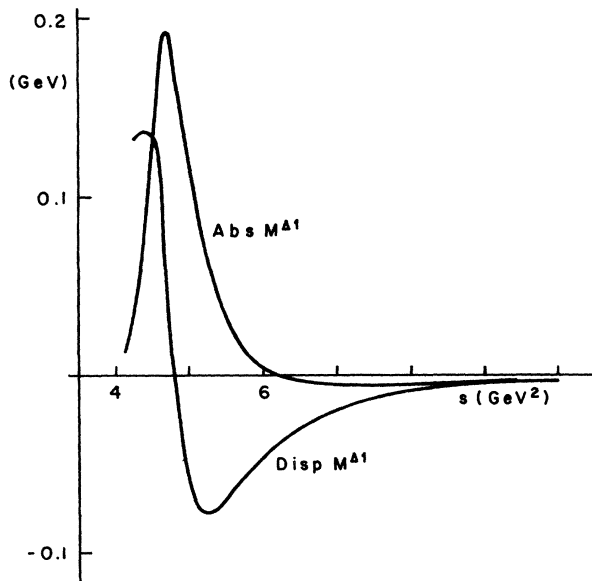


FIG. 5. Representation of the part of the vertex function for the diagram with an intermediate  $\Delta$  resonance which corresponds mainly to  $P$ -wave coupling of the  $\pi d$  system. The plotted quantities are defined through Eqs. (3.21) and (3.22).

where  $\vec{q}$  is the momentum of a nucleon in the NN c.m. frame;  $R_{kl}^{s_B}$  is the polarization tensor of a spin 2 particle; and  $T_1$ ,  $T_3$ , and  $T_B$  denote the isospin components of the two nucleons and of  $B_2$ , respectively.

With similar approximations and algebraic manipulations as for the intermediate  $\Delta$  contribution, we obtain at the end

$$\text{Abs} M_{s_d, s_B}^{\pi d B_2; N}(s) = R_{kl}^{s_B} 2 \left[ \frac{g_{\pi NN}}{2m_N} \right] g_{\text{NN}B_2} \left[ \frac{s}{4} - m_N^2 \right] \times \frac{(q_\pi)_k (q_\pi)_l}{|\vec{q}_\pi|^2} (\vec{q}_\pi \cdot \vec{\xi}^{s_d}) \text{Abs} M^N(s), \quad (4.3a)$$

with

$$\text{Abs} M^N(s) = \frac{i^3}{2i} \bar{P} \theta(s - 4m_N^2) \times \sum_{i=0}^n c_i [3I_2(\bar{A}_i, \bar{B}) - I_0(\bar{A}_i, \bar{B})]. \quad (4.3b)$$

The quantity  $g_{\pi NN}$  is the usual  $\pi NN$  coupling constant; the other quantities are defined as in the preceding section, except for

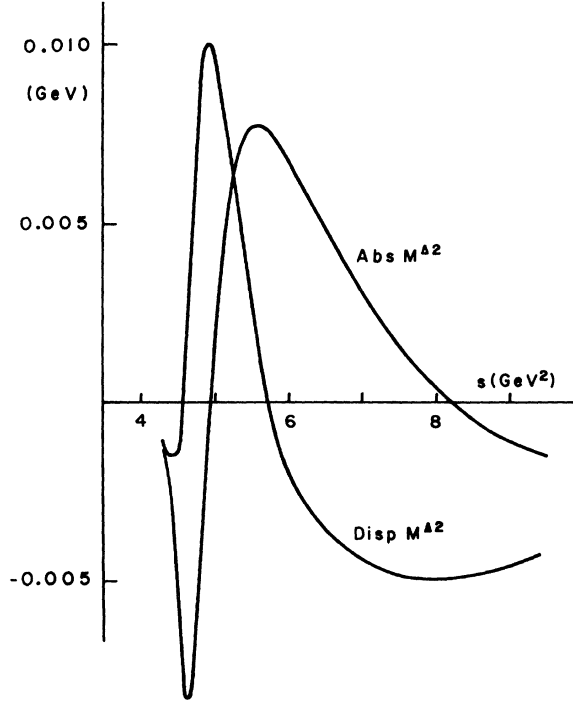


FIG. 6. Representation of the part of the vertex function for the diagram with intermediate  $\Delta$  line which corresponds to  $F$ -wave coupling of the  $\pi d$  system. The plotted quantities are defined through Eqs. (3.21) and (3.22). Notice the difference in scales between Figs. 5 and 6.

$$\begin{aligned}
 E_1 &= \sqrt{s}/2, \quad |\vec{q}_1| = (E_1^2 - m_N^2)^{1/2}, \\
 \bar{P} &= m_N^3 \frac{N_d}{2\pi |\vec{q}_d| \sqrt{s}}, \\
 \bar{A}_i &= m_d^2 - 2E_1 E_d - 2(\beta_i^2 - \beta_0^2), \\
 \bar{B} &= 2|\vec{q}_d| \cdot |\vec{q}_1|.
 \end{aligned}
 \tag{4.4}$$

The full amplitude is given by

$$\begin{aligned}
 M_{s_d, s_B}^{\pi d B_2; N}(s) &= R_{kl}^{s_B} 2 \left[ \frac{g_{\pi NN}}{2m_N} \right] g_{NNB} \left[ \frac{s}{4} - m_N^2 \right] \\
 &\quad \times \frac{(q_\pi)_k (q_\pi)_l}{|\vec{q}_\pi|^2} (\vec{q}_\pi \cdot \vec{\xi}^d) M^N(s),
 \end{aligned}
 \tag{4.5}$$

where

$$M^N(s) = \text{Disp} M^N(s) + i \text{Abs} M^N(s),
 \tag{4.6a}$$

with

$$\text{Disp} M^N(s) = \frac{1}{\pi} \int_{4m_N^2}^{\infty} \frac{\text{Abs} M^N(s')}{s' - s} ds'.
 \tag{4.6b}$$

The quantities  $\text{Abs} M^N(s)$  and  $\text{Disp} M^N(s)$  have practically the same values as  $\text{Abs} \hat{M}^N(s)$  and  $\text{Disp} \hat{M}^N(s)$  of Sec. II. Their general behavior can be observed in Fig. 3. We stress that the large suppression of the nucleon graph as compared to the  $\Delta$  graph is mainly due to the angular integrations implied by the  ${}^1D_2$  coupling of the two intermediate nucleons to the  $J^P=2^+$  dibaryon state. Due to this effect, the  $D$ -wave part of the deuteron wave function may become more significant for the case of two internal nucleons than it is for the case with intermediate  $\Delta$ .

## V. CONTRIBUTIONS TO $\pi$ -d AMPLITUDES

As a consequence of the preceding discussion, we can expect that the intermediate state  $\Delta N$  interaction noticeably affects the  $\pi d$  amplitudes and consequently the  $\pi d$  observables. In particular, dibaryonic resonant states coupled to the  $\Delta N$  system may be observed through their effects on the intermediate state in  $\pi d$  scattering. The contribution of the  $\Delta N$  interaction to the elastic  $\pi d$  scattering amplitudes is mainly determined by the skeleton diagram of Fig. 2. In treatments which deal with the  $\pi$ -d system as a system<sup>5</sup> of coupled  $\pi d$ ,  $NN\pi$ , and  $NN$  channels, the  $\Delta$  particle is not fully treated. Therefore a strong  $\Delta N$  interaction, which is suggested by the analysis of Refs. 3 and 4, is not properly taken care of in the existing calculations, and therefore the contribution of diagram 2 should be added to the background amplitudes evaluated in the conventional treatments.

As shown in the preceding sections, at intermediate energies the contributions of triangular diagrams with internal nucleon lines coupled to a  $J^P=2^+$  state are strongly suppressed. Their effects could therefore be neglected in a fair approximation to  $\pi$ -d scattering at these energies. Therefore the inclusion of the  $2^+$  resonance of two nucleons in the three-body treatment of  $\pi$ -d scattering will not give rise to significant signals of their presence. Observable dibaryon signals, however, may arise from a  $\Delta$ - $N$  interaction. This results from the enhancement of the  $\Delta$  graph near the  $\Delta N$  threshold, which is clearly shown in Fig. 5.

A crucial input to the  $\pi$ -d amplitude corresponding to the diagram in Fig. 2 is the matrix element describing the  $\Delta N$  interaction in the  $S$ -wave  $J=2$ ,  $I=1$  state, which we write as

$$\begin{aligned}
 M_{s_\Delta, s_N; s'_\Delta, s'_N}^{\Delta N \Delta N}(s) &= \sum_{s_B} \left\{ R_{kl}^{s_B} \sum_{ss'} [ \langle 1 \frac{1}{2}; ss' | 1 \frac{1}{2}; \frac{3}{2} s_\Delta \rangle [\chi^{s'}(-i\sigma_2 \sigma_k) \chi^{s_N}]_{\xi_l^{s'_\Delta}} R_{k'l'}^{s_B} \right. \\
 &\quad \left. \times \sum_{s''s'''} [ \langle 1 \frac{1}{2}; s''s''' | 1 \frac{1}{2}; \frac{3}{2} s'_\Delta \rangle [\chi^{s''}(\sigma_k i \sigma_2) \chi^{s'_N}]_{\xi_l^{s'''\Delta}} ] \right\} M^{\Delta N}(s).
 \end{aligned}
 \tag{5.1}$$

The notation is as in Eq. (3.8), with sums over  $k, k', l, l'$  indices assumed. The quantity  $M^{\Delta N}(s)$  is related to the  $\Delta N$  partial wave amplitude  $T_{ll'}^J$  through

$$M^{\Delta N}(s) = \frac{\pi}{m_N m_\Delta} \frac{\sqrt{s}}{2 |\vec{q}_\Delta|} T_{l=l'=0}^{J=2}(s), \quad (5.2a)$$

with

$$T_{l=l'=0}^{J=2}(s) = \frac{1}{2i} (\eta_{00}^2 e^{2i\delta_{00}^2} - 1), \quad (5.2b)$$

where  $\vec{q}_\Delta$  is the c.m. momentum of the  $\Delta N$  system.

We evaluate the matrix element corresponding to Fig. 2 with a  $\Delta N$  interaction in a  ${}^5S_2$ ,  $I=1$  state. We then find products of expressions already obtained for the vertex functions in Sec. III. The result is

$$M_{s_d s'_d}^{\pi d, \pi d; \Delta}(s) = \frac{64}{9} g_{\pi N \Delta}^2 M^{\Delta N}(s) \sum_{s_B} \left\{ R_{kl}^{s_B} \left[ (q_\pi)_k \xi_l^{s_d} M^{\Delta,1}(s) + M^{\Delta,2}(s) \frac{(q_\pi)_k (q_\pi)_l}{|\vec{q}_\pi|^2} (\vec{q}_\pi \cdot \vec{\xi}^{s_d}) \right] \right\} \\ \times \left\{ R_{k'l'}^{s_B} \left[ (q'_\pi)_{k'} \xi_{l'}^{s'_d} M^{\Delta,1}(s) + (\vec{\xi}^{*s'_d} \cdot \vec{q}'_\pi) \frac{(q'_\pi)_{k'} (q'_\pi)_{l'}}{|\vec{q}_\pi|^2} M^{\Delta,2}(s) \right] \right\}, \quad (5.3)$$

where  $\vec{q}_\pi$  and  $\vec{q}'_\pi$  are the  $\pi$  momentum in the c.m. frame in the initial and final states, respectively.

We sum over the 3-components of the spins of the  $J=2^+$  amplitude, using the following normalization for the polarization tensor:

$$\sum_{s_B} R_{kl}^{s_B} R_{k'l'}^{s_B} = \delta_{kk'} \delta_{ll'} + \delta_{kl'} \delta_{k'l} - \frac{2}{3} \delta_{kl} \delta_{k'l'}, \quad (5.4)$$

and obtain

$$M_{s_d s'_d}^{\pi d, \pi d; \Delta}(s) = \frac{64}{9} g_{\pi N \Delta}^2 M^{\Delta N}(s) \left\{ (\vec{q}_\pi \cdot \vec{q}'_\pi) (\vec{\xi}^{*s'_d} \cdot \vec{\xi}^{s_d}) (M^{\Delta,1}(s))^2 + (\vec{\xi}^{*s'_d} \cdot \vec{q}_\pi) (\vec{q}'_\pi \cdot \vec{\xi}^{s_d}) (M^{\Delta,1}(s))^2 \right. \\ \left. - \frac{2}{3} (\vec{\xi}^{*s'_d} \cdot \vec{q}'_\pi) (\vec{q}_\pi \cdot \vec{\xi}^{s_d}) [M^{\Delta,1}(s) + M^{\Delta,2}(s)]^2 + 2 (\vec{\xi}^{*s'_d} \cdot \vec{q}'_\pi) (\vec{q}_\pi \cdot \vec{\xi}^{s_d}) \frac{(\vec{q}_\pi \cdot \vec{q}'_\pi)^2}{|\vec{q}_\pi|^4} (M^{\Delta,2}(s))^2 \right. \\ \left. + 2 [(\vec{\xi}^{*s'_d} \cdot \vec{q}'_\pi) (\vec{q}'_\pi \cdot \vec{\xi}^{s_d}) + (\vec{\xi}^{*s'_d} \cdot \vec{q}_\pi) (\vec{q}_\pi \cdot \vec{\xi}^{s_d})] \frac{(\vec{q}_\pi \cdot \vec{q}'_\pi)}{|\vec{q}_\pi|^2} M^{\Delta,1}(s) M^{\Delta,2}(s) \right\}, \quad (5.5)$$

For the evaluation of  $\pi d$  observables we require the contributions of this matrix element to the helicity scattering amplitudes  $f_{\lambda'\lambda}(\theta)$ , where  $\lambda'$ ,  $\lambda$  represent the final and initial helicity, respectively, and  $\theta$  is the scattering angle in the c.m. frame. These contributions are the following:

$$f_{++}(\theta) = \frac{1}{8\pi\sqrt{s}} \langle + | M_{s_d s'_d}^{\pi d, \pi d; \Delta}(s) | + \rangle = \frac{8}{9\pi\sqrt{s}} g_{\pi N \Delta}^2 M^{\Delta N}(s) |\vec{q}_\pi|^2 (M^{\Delta,1}(s))^2 d_{11}^2(\theta), \\ f_{00}(\theta) = \frac{1}{8\pi\sqrt{s}} \langle 0 | M_{s_d s'_d}^{\pi d, \pi d; \Delta}(s) | 0 \rangle = \frac{8}{9\pi\sqrt{s}} g_{\pi N \Delta}^2 M^{\Delta N}(s) |\vec{q}_\pi|^2 \frac{4}{3} (M^{\Delta,1}(s) + M^{\Delta,2}(s))^2 d_{00}^2(\theta), \\ f_{+-}(\theta) = \frac{1}{8\pi\sqrt{s}} \langle + | M_{s_d s'_d}^{\pi d, \pi d; \Delta}(s) | - \rangle = \frac{8}{9\pi\sqrt{s}} g_{\pi N \Delta}^2 M^{\Delta N}(s) |\vec{q}_\pi|^2 (M^{\Delta,1}(s))^2 d_{-11}^2(\theta), \\ f_{+0}(\theta) = \frac{1}{8\pi\sqrt{s}} \langle + | M_{s_d s'_d}^{\pi d, \pi d; \Delta}(s) | 0 \rangle = \frac{8}{9\pi\sqrt{s}} g_{\pi N \Delta}^2 M^{\Delta N}(s) |\vec{q}_\pi|^2 \frac{2}{\sqrt{3}} M^{\Delta,1}(s) (M^{\Delta,1}(s) + M^{\Delta,2}(s)) d_{01}^2(\theta). \quad (5.6)$$

We have thus given expressions for the corrections, due to the  $\Delta N$  interaction in the intermediate  $J=2$  state, to the helicity scattering amplitudes of  $\pi d$  elastic scattering in terms of known quantities and of the  ${}^5S_2$ ,  $I=1$ ,  $\Delta N$  partial amplitude. We stress that the results expressed by Eqs. (5.6) are independent of assumptions about the existence of a  $J^P=2^+$  dibaryon resonance, which would enter through a specific structure to be given to the quan-

tity  $M^{\Delta N}(s)$ . With these expressions at hand we may test the consistency between the coupled channel analyses which determine  $M^{\Delta N}(s)$  and the  $\pi d$  scattering data. These applications require further investigation.

This work was partially supported by DAAD, Financiadora de Estudos e Projetos (FINEP), and Conselho Nacional de Pesquisas (CNPq).

- <sup>1</sup>Particle Data Group, Review of Particle Properties, April 1982 ed.
- <sup>2</sup>A. Yokosawa, Phys. Rep. 64, 47 (1980); N. Hoshizaki, Prog. Theor. Phys. 60, 1796 (1978); 61, 129 (1979).
- <sup>3</sup>B. J. Edwards and G. H. Thomas, Phys. Rev. D 22, 2772 (1980); B. J. Edwards, *ibid.* 23, 1978 (1981).
- <sup>4</sup>I. L. Grach, I. M. Narodetskii, and M. Zh. Shmatikov, ITEP (USSR) report, 1983.
- <sup>5</sup>B. Blankleider and I. R. Afnan, Phys. Rev. C 24, 1572 (1981); C. Fayard, G. H. Lamot, and T. Mizutani, Phys. Rev. Lett. 45, 524 (1980); N. Giraud, C. Fayard, and G. H. Lamot, Phys. Rev. C 21, 1959 (1980); A. S. Rinat and Y. Starkand, Nucl. Phys. A397, 381 (1983).
- <sup>6</sup>K. Kanai *et al.*, Prog. Theor. Phys. 62, 153 (1979); K. Kubodera *et al.*, J. Phys. G 6, 171 (1980); C. Fayard *et al.*, Phys. Rev. Lett. 45, 524 (1980); A. Matsuyama and K. Yasaki, Nucl. Phys. A364, 477 (1981); E. Ferreira and G. Perez, J. Phys. G 9, 169 (1983); M. P. Locher and M. E. Sainio, Phys. Lett. 121B, 227 (1983).
- <sup>7</sup>A. Matsuyama and K. Yazaki, Nucl. Phys. A364, 477 (1981).
- <sup>8</sup>I. J. McGee, Phys. Rev. 151, 151 (1966).
- <sup>9</sup>H. G. Dosch, S. C. B. de Andrade, E. Ferreira, and G. Perez Munguia, Phys. Rev. C 29, 1549 (1984).
- <sup>10</sup>R. E. Cutkosky, J. Math. Phys. 1, 429 (1960).